

## Research Article

# Design of Joint Spatial and Power Domain Multiplexing Scheme for Massive MIMO Systems

**Zheng Jiang, Bin Han, Peng Chen, Fengyi Yang, and Qi Bi**

*Technology Innovation Center, China Telecom Corporation Limited, China Telecom Beijing Information Science and Technology Innovation Park, Southern Zone of Future Science and Technology City, Beiqijia, Changping, Beijing 102209, China*

Correspondence should be addressed to Zheng Jiang; [jiangzh@ctbri.com.cn](mailto:jiangzh@ctbri.com.cn)

Received 14 August 2015; Accepted 15 October 2015

Academic Editor: Wei Xiang

Copyright © 2015 Zheng Jiang et al. This is an open access article distributed under the Creative Commons Attribution License, which permits unrestricted use, distribution, and reproduction in any medium, provided the original work is properly cited.

Massive Multiple-Input Multiple-Output (MIMO) is one of the key techniques in 5th generation wireless systems (5G) due to its potential ability to improve spectral efficiency. Most of the existing works on massive MIMO only consider Time Division Duplex (TDD) operation that relies on channel reciprocity between uplink and downlink channels. For Frequency Division Duplex (FDD) systems, with continued efforts, some downlink multiuser MIMO scheme was recently proposed in order to enable “massive MIMO” gains and simplified system operations with limited number of radio frequency (RF) chains in FDD system. However these schemes, such as Joint Spatial Division and Multiplexing (JSDM) scheme and hybrid precoding scheme, only focus on multiuser transmission in spatial domain. Different from most of the existing works, this paper proposes Joint Spatial and Power Multiplexing (JSPM) scheme in FDD systems. It extends existing FDD schemes from spatial division and multiplexing to joint spatial and power domain to achieve more multiplexing gain. The user grouping and scheduling scheme of JSPM is studied and the asymptotic expression for the sum capacity is derived as well. Finally, simulations are conducted to illustrate the effectiveness of the proposed scheme.

## 1. Introduction

With increasing popularity of smart phones, pads, and tablet computers, mobile data traffic is experiencing unprecedented growth. Mobile broadband networks need to support explosively growing consumer data rate demands and need to tackle the exponential increase in the predicted traffic volumes. An efficient radio access technology combined with higher spectrum efficiency is essential to achieve the growing demands faced by wireless carriers. Massive MIMO is one of the core technologies expected to be adopted by the next generations of wireless communication systems. With massive MIMO, plenty of user equipment (UE) can be served simultaneously by the system with the antenna array of a few hundred antennas on the same time-frequency resource [1, 2].

Massive MIMO relies on spatial multiplexing to make advantages over conventional passive antenna system, which needs the base station (BS) to have accurate channel knowledge on both the uplink and the downlink. On the uplink, it is easy to accomplish this by letting the UE send pilots, based on

which BS estimates the channel responses to the UE. On the downlink, in conventional MIMO systems such as Long Term Evolution (LTE) system, BS sends cell reference signals (CRS) or/and Channel State Information Reference Signals (CSI-RS), based on which UE estimates the channel responses, quantizes the obtained channel estimates, and feeds them back to the BS. Since the amount of time-frequency resources needed for downlink reference signals is proportional to the number of antennas and the amount of uplink channel state information (CSI) feedback resources is proportional to the number of active users, a massive MIMO system may require up to tens of times more resources than a conventional system. Due to this, the massive MIMO is more likely to be applied in TDD systems which rely on reciprocity between the uplink and downlink channels [3–5].

On the other hand, considerable effort has been dedicated to study the implementation of massive MIMO in FDD systems with various practical constraints, including nonideal CSI at the transmitter [6], the overhead incurred by downlink channel probing, and CSI feedback [7, 8]. Joint

Spatial Division and Multiplexing (JSDM) was proposed in [9–11] to enable massive MIMO gains for FDD systems. Meanwhile, as large bandwidth is available at millimeter wave (mmWave) frequencies to provide gigabit-per-second data rates, the hybrid analog/digital processing strategies were proposed in [12–15] for mmWave systems with large antenna arrays.

The downlink beamforming of both JSDM and hybrid precoding scheme includes two stages, that is, a prebeamforming stage that depends on UE's channel covariance and a MU-MIMO precoding stage for the effective channel formed by the first stage. The prebeamforming matrix is chosen in order to minimize the interference across different spatial groups, and the MU-MIMO precoding matrix takes care of the multiuser interference within each group.

Both of these beamforming stages achieve multiplexing gain in spatial domain. It is well-known that the maximum spatial multiplexing gain is limited by the number of transmitting and receiving antennas in massive MIMO systems [16]. Thus, more multiplexing gain is achieved in the first prebeamforming stage; the less multiplexing gain is achieved in the second MU-MIMO stage. In order to achieve more multiplexing gain in the MU-MIMO stage, the power domain is introduced in spatial multiplexing transmission scheme and the joint spatial and power multiplexing (JSPM) scheme for massive MIMO system is proposed in this paper. The proposed scheme not only relaxes the full channel knowledge to achieve the spatial multiplexing gain by using the channel second order statistics, but also applies multiuser power allocation transmission at BS side and successive interference canceller (SIC) on UE side to achieve the power-domain user multiplexing gain. The performance of the proposed JSPM scheme is illustrated by simulations and compared with that of JSDM. The results show that even with the fixed spatial quantization and simplified transmit power allocation grouping scheme, the proposed scheme outperforms JSDM because of the additional power-domain multiplexing gain.

The remainder of this paper is organized as follows: Section 2 describes the overall system model and the key functionalities utilized to introduce JSPM. The asymptotic expression of JSPM is derived. Section 3 discusses the scheme of the user spatial grouping and multiuser power-domain paring. Furthermore the computational complexity of JSPM scheme is discussed. In Section 4, the system-level simulation configuration is described and the results of the system-level performance of JSPM in comparison to JSDM are provided. Finally, Section 5 concludes the paper.

## 2. System Model

In this section, we consider the downlink communication of a massive MIMO system as shown in Figure 1, where the base station (BS) is equipped with  $N_t$  transmit antennas under the total transmit power constraint of  $P$  and serving  $U$  signal antenna UE.

We assume that  $\mathbf{H} = [\mathbf{h}_1, \dots, \mathbf{h}_u, \dots, \mathbf{h}_U]$  is the  $N_t \times U$  dimensional matrix that represents the channel between the BS and UE,  $\mathbf{h}_u$  is the  $N_t \times 1$  dimensional channel realization between the BS and user  $u$ .

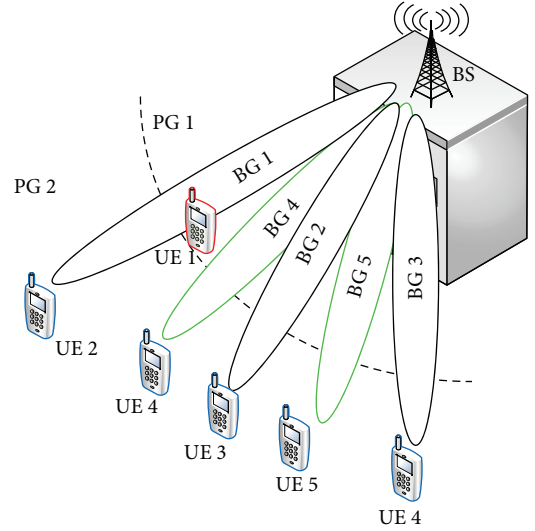


FIGURE 1: A massive MIMO BS to serve randomly located UE.

The system received signal is denoted as

$$\mathbf{y} = \mathbf{H}^H \mathbf{x} + \mathbf{n}, \quad (1)$$

where  $\mathbf{y}$  denotes the collection of received symbols for all the  $U$  users,  $\mathbf{x} = \mathbf{T}\mathbf{d}$  is the transmitted signal vector of dimensions  $N_t \times 1$ ,  $\mathbf{T} = \mathbf{BVP}$  is the downlink beamforming matrix consisting of three parts:  $\mathbf{B}$  is the prebeamforming matrix of dimensions  $N_t \times N_B$ , which is generated based on the channel covariance statistics;  $\mathbf{V}$  is the  $N_B \times N_M$  multiuser MIMO precoding matrix which is a function of the reduced dimensional effective channel  $\bar{\mathbf{H}} = \mathbf{B}^H \mathbf{H}$ ;  $\mathbf{P}$  is the power-domain multiplexing matrix of dimensions  $N_M \times N_S$ ;  $\mathbf{d}$  denotes the  $S \times 1$  vector of transmitted user data symbols.  $\mathbf{n} \sim \mathcal{CN}(0, \mathbf{I}_{U_k})$  denotes additive spatially and temporally white Gaussian noise with zero mean and unit variance. As a result, the received signal in (1) can be written in the following manner:

$$\mathbf{y} = \mathbf{H}^H \mathbf{BVPd} + \mathbf{n} = \bar{\mathbf{H}}^H \mathbf{VPd} + \mathbf{n}, \quad (2)$$

where prebeamforming matrix  $\mathbf{B}$  makes the channel  $\mathbf{H}$  become different approximately mutually orthogonal subspaces  $\bar{\mathbf{H}}$  based on channel statistical characteristic, UE can be partitioned into these subspaces to form several disjoint user groups.

If we define  $U$  users can be partitioned into  $G$  groups; the overall  $N_t \times U$  system channel matrix  $\mathbf{H} = [\mathbf{H}^1 \ \dots \ \mathbf{H}^G]$ ;  $\mathbf{H}^g$  is the  $N_t \times U^g$  channel matrix of users in group  $g$ ,  $\sum_{g=1}^G U^g = U$ . Prebeamforming matrix  $\mathbf{B} = [\mathbf{B}^1 \ \dots \ \mathbf{B}^G]$ ;  $\mathbf{B}^g$  denotes the  $N_t \times U^g$  prebeamforming matrix of group  $g$ ,  $\sum_{g=1}^G U^g = U$ .

Then we have

$$\bar{\mathbf{H}} = \mathbf{H}^H \mathbf{B} = \begin{pmatrix} (\mathbf{H}^1)^H \mathbf{B}^1 & \dots & (\mathbf{H}^1)^H \mathbf{B}^G \\ \vdots & \ddots & \vdots \\ (\mathbf{H}^G)^H \mathbf{B}^1 & \dots & (\mathbf{H}^G)^H \mathbf{B}^G \end{pmatrix}, \quad (3)$$

the received signal for users in group  $g$ ,

$$\mathbf{y}^g = (\mathbf{H}^g)^H \mathbf{B}^g \mathbf{V}^g \mathbf{P}^g \mathbf{d}^g + \sum_{g'=1, g' \neq g}^G (\mathbf{H}^g)^H \mathbf{B}^{g'} \mathbf{V}^{g'} \mathbf{P}^{g'} \mathbf{d}^{g'} + \mathbf{n}^g. \quad (4)$$

Based on [11],  $\mathbf{H}^g = \mathbf{U}^g (\Lambda^g)^{1/2} \mathbf{w}^g$ . Then we can make the effective channel matrix  $\bar{\mathbf{H}}$  become an approximate block diagonal matrix by designing  $\mathbf{B}^g = \mathbf{U}^g$ , then  $(\mathbf{H}^g)^H \mathbf{B}^{g'} \approx 0$  where  $g, g' \in \{1, \dots, G\}$  and  $g \neq g'$ . Furthermore, the  $\mathbf{y}^g$  in (4) can be expressed as

$$\mathbf{y}^g \approx \bar{\mathbf{H}}^g \mathbf{V}^g \mathbf{P}^g \mathbf{d}^g + \mathbf{n}^g = \mathbf{w}^g (\Lambda^g)^{1/2} \mathbf{V}^g \mathbf{P}^g \mathbf{d}^g + \mathbf{n}^g, \quad (5)$$

where  $\mathbf{V}^g$  and  $\mathbf{P}^g$  are the multiuser MIMO precoding matrix and the power-domain multiplexing matrix of user cluster  $g$ , respectively,  $\mathbf{d}^g$  is the transmitted signal of cluster  $g$ , and  $\mathbf{n}^g \sim \text{CN}(0, \mathbf{I}^g)$ . From (5), we can derive that  $\mathbf{V}$  is the block diagonal matrix,  $\mathbf{V} = \text{diag}(\mathbf{V}^1, \dots, \mathbf{V}^G)$ .

The number of downlink data streams of group  $g$  is denoted as  $r^g$  which is the effective rank of  $\mathbf{R}^g$ , and MU-MIMO precoding matrix in group  $g$  is simply the identity matrix; that is,  $\mathbf{V}^g = \mathbf{I}^{r^g}$ . In order to allocate the downlink data streams to the users, we select  $r^g$  out of users in  $U^g$ , which is the number of users in group  $g$ , according to a max SINR criterion as follows:

$$\text{SINR}_{u,m}^g = \frac{|(h_u^g)^H (b_m^g)|^2}{1/\rho + \sum_{n \neq m} |(h_u^g)^H (b_n^g)|^2 + \sum_{g' \neq g} \left\| (h_u^g)^H (\mathbf{B}^{g'}) \right\|^2}, \quad (6)$$

where  $m = 1, \dots, r^g$ ,  $b_m^g, b_n^g$  is the  $m$ th and  $n$ th column of  $\mathbf{B}^g$ ,  $h_u^g$  is the channel response vector of user  $u$  in spatial group  $g$ , and  $\rho = P / \sum_{g=1}^G r^g$ .

Each user feeds its SINR values and  $m$ th beam index corresponding to this SINR back. BS can then identify each type of UE by a set of indices  $\{u, g, m\}$  where indices  $\{u, g, m\}$  are the user index, spatial group number which user  $u$  belongs to, and beam index corresponding to  $\text{SINR}_{u,m}^g$ , respectively.

In addition to these indices, a new index, introduced in JSMP to identify UEs, is the power-domain group index, which can be decided based on RSRP value of UE feedback and the predefined thresholds. For example, we can predefine several intervals of RSRP as different power groups; if a UE feedback RSRP value is in  $d$ th RSRP interval, the UE is considered to belong to power group  $d$ .

For UE with a different power group index  $d$  and the same beam index  $m$ , UE can be paired to use power-domain multiplexing; the presentation is

$$\mathbf{s}^g = \mathbf{P}^g \mathbf{d}^g, \quad (7)$$

where  $\mathbf{s}^g = [\mathbf{s}_1^g, \dots, \mathbf{s}_{r^g}^g]$  is  $r^g$  transmission data streams.  $\mathbf{P}^g$  with dimensions  $r^g \times U^g$  is power-domain multiplexing matrix to multiplex  $U^g$  user data into  $r^g$  data stream.  $\mathbf{d}^g = [\mathbf{d}_1^g, \dots, \mathbf{d}_{U^g}^g]$  is the data vector of  $U^g$  users in group  $g$ .

There are two criteria of power-domain multiuser scheduler as follows.

The first is the fact that multiplexing candidate users will be selected from UE set with the same spatial group index  $g$  and beam index  $m$ , but with different power-domain group index. For example, if user  $u'$  and user  $u$  are two selected users to multiuser transmission in power domain, they will be allocated in different power groups, such as user  $u' \in U_{m,d'}^g$  and user  $u \in U_{m,d}^g$ ; variables  $d'$  and  $d$  are different power group indices;  $U_m^g$  is the user set of spatial group  $g$  and beam  $m$ .

The second is the multiplexing candidate user that will maximize the PF scheduling metric as follows:

$$Q_{U_m^g} = \sum_{u \in U_m^g} \left( \frac{R(u)}{\bar{R}(u)} \right), \quad (8)$$

where  $Q_{U_m^g}$  denotes the PF scheduling metric for power-domain multiplexing candidate user set  $U_m^g$ ;  $R(u)$  is the instantaneous throughput of user  $u$ ;  $\bar{R}(u)$  is the average throughput of user  $u$ .

We assume that the SIC receiver of user  $u$  is able to cancel perfectly and successively the interference from other user  $w$  with channel gain  $P_u^g |(h_u^g)^H (b_m^g)|^2 > P_w^g |(h_u^g)^H (b_m^g)|^2$ ,  $u \in U_{m,d}^g$ , and  $u' \in U_{m,d'}^g$ . Then SINR of user  $u$  can be estimated by

$$\text{SINR}_{u,m,d}^g = \frac{P_u^g |(h_u^g)^H (b_m^g)|^2}{I_{u',m,d'}^g + P_u^g \left( \sum_{n \neq m} |(h_u^g)^H (b_n^g)|^2 + \sum_{g' \neq g} \left\| (h_u^g)^H (\mathbf{B}^{g'}) \right\|^2 \right) + 1}, \quad (9)$$

where

$$I_{u',m,d'}^g = \sum_{\substack{P_{u'}^g |(h_{u'}^g)^H (b_m^g)|^2 \leq P_u^g |(h_u^g)^H (b_m^g)|^2, u' \neq u}} P_{u'}^g |(h_{u'}^g)^H (b_m^g)|^2 \quad (10)$$

and  $u \in U_{m,d}^g$ ,  $u' \in U_{m,d'}^g$ , and  $u, u' \in U_m^g$  and  $P_{u,d}^g$  is the allocated power of user  $u$  in spatial group  $g$ .

If we assume  $l_m^g$  is the power-domain multiplexing user number in user set  $U_m^g$ ,  $l_m^g$  is less than or equal to the number of power-domain groups. In the derivation of an asymptotic expression,  $l_m^g$  is assumed to be equal to the number of power-domain group. The data stream number of spatial group  $g$  can be expressed as  $L^g = \sum_{m=1}^{r^g} l_m^g$ .

With this user selection and data stream multiplexing scheme, the sum rate of group  $g$  is given by

$$R^g = \sum_{m=1}^{r^g} \sum_{d=1}^{l_m^g} E \left[ \log \left( 1 + \max_{1 \leq u \leq U^g} \text{SINR}_{u,m,d}^g \right) \right]. \quad (11)$$

The CDF of  $\text{SINR}_{u,m,d}^g$  is given by

$$F(X) = 1 - P(\text{SINR}_{u,m,d}^g > x). \quad (12)$$

Using (9) into (12), we can write the SINR CDF as

$$F(X) = 1 - P(Z_{u,m,d}^g > 0), \quad (13)$$

where

$$\begin{aligned} Z_{u,m,d}^g = & \left| (\omega_u^g)^H (\Lambda^g)^{1/2} (U^g)^H b_m^g \right|^2 - x \left[ \frac{1 + I_{u',m,d'}^g}{P_u^g} \right. \\ & + \sum_{n \neq m} \left| (\omega_u^g)^H (\Lambda^g)^{1/2} (U^g)^H b_n^g \right|^2 \\ & \left. + \sum_{g' \neq g} \left\| (\omega_u^g)^H (\Lambda^g)^{1/2} (U^g)^H B^{g'} \right\|^2 \right]. \end{aligned} \quad (14)$$

Then following the analysis of [11, 17],

$$F(X) = 1 - \frac{e^{-x/\delta_d \mu_{m,1}^g(x)}}{\prod_{j=2}^{r_g} (1 - \mu_{m,j}^g(x) / \mu_{m,1}^g(x))}, \quad (15)$$

where  $\mu_{m,j}^g(x)$ ,  $j = 1, \dots, r_g$  are the eigenvalues of  $A_m^g(x)$ ,

$$\begin{aligned} A_m^g(x) = & (\Lambda^g)^{1/2} (U^g)^H b_m^g (b_m^g)^H U^g (\Lambda^g)^{1/2} \\ & - x \left( \sum_{n \neq m} (\Lambda^g)^{1/2} (U^g)^H b_n^g (b_n^g)^H U^g (\Lambda^g)^{1/2} \right. \\ & \left. + \sum_{g' \neq g} (\Lambda^g)^{1/2} (U^g)^H B^{g'} (B^{g'})^H U^g (\Lambda^g)^{1/2} \right). \end{aligned} \quad (16)$$

Without loss of generality, we assume the ordering

$$\begin{aligned} \mu_{m,1}^g(x) \geq & \dots \geq \mu_{m,r_g}^g(x), \\ \delta_d = & \frac{P_u^g}{1 + I_{u',m,d'}^g}. \end{aligned} \quad (17)$$

The growth function of CDF  $F(x)$  with corresponding PDF  $f(x)$  is

$$\begin{aligned} g(x) = & \frac{1 - F(x)}{f(x)}, \\ g^\infty = & \lim_{x \rightarrow \infty} g(x) = \delta_d (\mu_{m,1}^g)^\infty, \end{aligned} \quad (18)$$

where  $(\mu_{m,1}^g)^\infty = \lim_{x \rightarrow \infty} \mu_{m,1}^g(x)$  is a bound positive constant [11].

Considering the ideal channel estimation and the fixed power assignments to users,  $I_{u,m,d}^g \rightarrow 0$ ,  $\delta_d \rightarrow P_d^g$ .

Then we have

$$\sum_{d=1}^{l_m^g} P_d^g = P^g. \quad (19)$$

With extreme value theory [11], we have that  $\max_{1 \leq u \leq U^g} \text{SINR}_{u,m,d}^g$  which behaves as  $\delta_d (\mu_{m,1}^g)^\infty \log U^g + O(\log \log U^g)$  for  $U^g \rightarrow \infty$ .

The sum rate asymptotic formula for a group  $g$  is

$$\begin{aligned} R_g = & \sum_{m=1}^{r_g} \sum_{d=1}^{l_m^g} \log(\delta_d (\mu_{m,1}^g)^\infty \log(U^g)) + o(1) \\ = & \sum_{m=1}^{r_g} \sum_{d=1}^{l_m^g} \log(\delta_d) + \sum_{m=1}^{r_g} \sum_{d=1}^{l_m^g} (\mu_{m,1}^g)^\infty \\ & + \sum_{m=1}^{r_g} \sum_{d=1}^{l_m^g} \log \log(U^g) + o(1) \\ = & \sum_{m=1}^{r_g} \sum_{d=1}^{l_m^g} \log(P_d^g) + \sum_{m=1}^{r_g} l_m^g \log \log(U^g) \\ & + \sum_{m=1}^{r_g} l_m^g \log(\mu_{m,1}^g)^\infty + o(1) \end{aligned} \quad (20)$$

as  $U^g \rightarrow \infty$ .

Summing over  $g$ , the sum rate asymptotic formula can be written as

$$\begin{aligned} R_{\text{sum}} = & \sum_{g=1}^G \sum_{d=1}^{l_m^g} r^g \log(P_d) + \sum_{g=1}^G L^g \log \log(U^g) \\ & + O(1). \end{aligned} \quad (21)$$

With finite  $N_t$  antennas, total transmit power constraint of  $P$ ,  $U^g$  users, and  $L^g$  data streams per group with the equal transmission power and common covariance  $\mathbf{R}^g$  where users have mutually statistically independent channel vectors, for  $U^g \rightarrow \infty$ , the sum capacity of a MU-MIMO downlink system is given by

$$\begin{aligned} R_{\text{sum}} = & \sum_{g=1}^G L^g \left[ \log \log(U^g) + \log \left( \frac{P}{\sum_{g=1}^G L^g} \right) \right] \\ & + O(1), \end{aligned} \quad (22)$$

where  $O(1)$  denotes a constant, independent of  $U^g$ .

### 3. Designs for JSPM in FDD

In the proposed JSPM scheme, the downlink transmission strategy is designed in the following three parts:

- (1) Based on cell environment and channel covariance measurement, BS can split whole channel space into several disjoint subspaces by using prebeamforming matrix. Therefore based on CSI, SINR, and RSRP values feedback from UE that estimates these values based on the subspaces, BS can partition its serving UE into several subspace groups with approximately similar channel covariance eigenvectors and channel path loss. The spatial and power-domain characters of each type of UE can be identified by a set of indices; that is, {UE index  $u$ , spatial group index  $g$ , beam index  $m$ , power group index  $d$ }.



- (2) For UE marked with different spatial group indices or the same spatial group index but different beam indices, MU-MIMO downlink transmission on the same time-frequency resource is performed.
- (3) For UE marked with the same spatial group index, the same beam index, and different power group indices, multiuser power pairing is performed. If user pairing succeeds, the multiuser power allocation and the power-domain user multiplexing transmission are performed.

Among the above, the user grouping and multiuser selection in power-domain are two key issues for the system performance; the following discussion will focus more on the strategies of these two issues.

**3.1. User Grouping.** As mentioned before, in order to exploit effectively the JSPM approach, the users' population will be partitioned into groups according to the following qualitative principles: (1) users in the same group have channel covariance eigenspace spanning (approximately) a given common subspace, which characterizes the spatial group; BS can get this information by UE CSI, SINR, and RSRP measurement feedback; (2) the subspaces of spatial groups served on the same time-frequency slot by JSDM must be (approximately) mutually orthogonal or at least have empty intersection.

The fixed quantization algorithm of user grouping in [11] is an effective and low complexity scheme for application in practical network. In this algorithm, the group subspaces are fixed a priori based on the geometry of cell coverage and their channel scattering. In our proposed scheme, the fixed quantization algorithm in [11] is extended to frequency domain. When we increase the number of fixed quantization spatial group to reduce coverage holes, the overlapping between different spatial groups will also increase and cause the strong interference of intergroups. In this case, we can allocate transmission resource in different frequency bands dynamically for UE that belongs to adjacent groups in order to reduce the interference of intergroups.

By choosing  $G$  AoAs  $\theta^g$  and fixed  $AS\Delta$ , we can define the  $G$  disjoint intervals  $[\theta^g - \Delta, \theta^g + \Delta]$ . This method consists essentially to form predefined "narrow sectors" and associate users to sectors according to minimum chordal distance quantization. For example, suppose  $G = 3$ , choosing  $\theta^1 = -45^\circ$ ,  $\theta^2 = 0^\circ$ , and  $\theta^3 = 45^\circ$ ,  $\Delta = 15^\circ$ , such as BG1, BG2, and BG3 shown in Figure 1, we note that the three subspaces are disjoint. However, as UE is distributed uniformly and these three subspaces are discontinuous, some UE cannot be associated with these subspaces exactly, such as UE4 shown in Figure 1. If we define more dense subspace such as  $G = 5$ , there are five spatial groups, such as BG1, BG2, ..., BG5 shown in Figure 1, and different subspace will be overlapping, the interference of inter-group will increase. In this case, we can allocate UE that is in the adjacent subspace to different frequency resources in order to reduce the intergroup interference.

In Figure 1, there are five spatial groups, in order to avoid intergroup interference, BS can separate BG1, BG2, and BG3

groups and BG4 and BG5 groups into different frequency bands.

This scheme makes sense especially for mmWave mobile systems which have huge frequency broadband to be used.

**3.2. Multiuser Transmit Power Allocation and Candidate User Selection.** Due to power-domain multiuser multiplexing, the transmit power allocation to one user affects the achievable throughput of not only that user but also the throughput of other pairing users. The best performance of power-domain multiuser multiplexing is achieved by exhaustive full search of user pairs and transmission power allocations [18].

In order to reduce further the computational complexity, the scheme of predefined user grouping and pergroup fixed power allocation can be used. With this approach, UE is divided into different user groups according to their channel path loss and the predefined thresholds. In this predefined power-domain grouping, the users can be paired together only if they belong to different power groups. With the predefined power grouping, the power allocation could also be simplified by applying fixed power assignments to the users belonging to the same group. For example, for the user group with good channel gain, small power (e.g., 0.3P) is allocated and, for the user group with bad channel gain, large power (e.g., 0.7P) is allocated, where the total power assigned to different user groups is kept equal to P. Predefined user grouping and fixed power allocation can effectively decrease the amount of downlink signaling related to UE data detection. For example, the order of successive interference cancellation (SIC) and information on power assignment do not need to be transmitted in every subframe but rather on a larger time scale.

For example, as shown in Figure 2, there are two spatial groups BG1 and BG2 and two power groups PG1 and PG2; UE1 belongs to BG1 and PG1 and UE2 and UE3 belong to BG1 and BG2, respectively, but both belong to PG2. As for the aforementioned spatial and power-domain multiplexing strategies, UE3 can be paired with UE1 and UE2 in the spatial domain and be applied to MU-MIMO transmission. UE1 can be paired with UE2 in power domain as it belongs to same spatial group but different power groups and it can be applied to multiuser power multiplexing transmission. UE1 can perform SIC operation to cancel the interference from UE2.

**3.3. Computational Complexity Discussion.** As multiuser transmission of power domain introduced in JSPM will lead to additional algorithm implementation complexity, we will discuss the computational complexity of JSPM in comparison with the exiting JSDM scheme in this section. The additional implementation complexity of JSDM is composed of three parts: the first part is multiuser selection and pairing in power domain in BS side, the second part is multiplexing transmission processing in power domain in BS side, and the third part is SIC processing in UE side. The first two parts increase the implementation complexity of BS side, and the last part increases the complexity of UE side.

In order to simplify complexity analysis, we assume that UE in power domain is separated into two groups, that is, cell

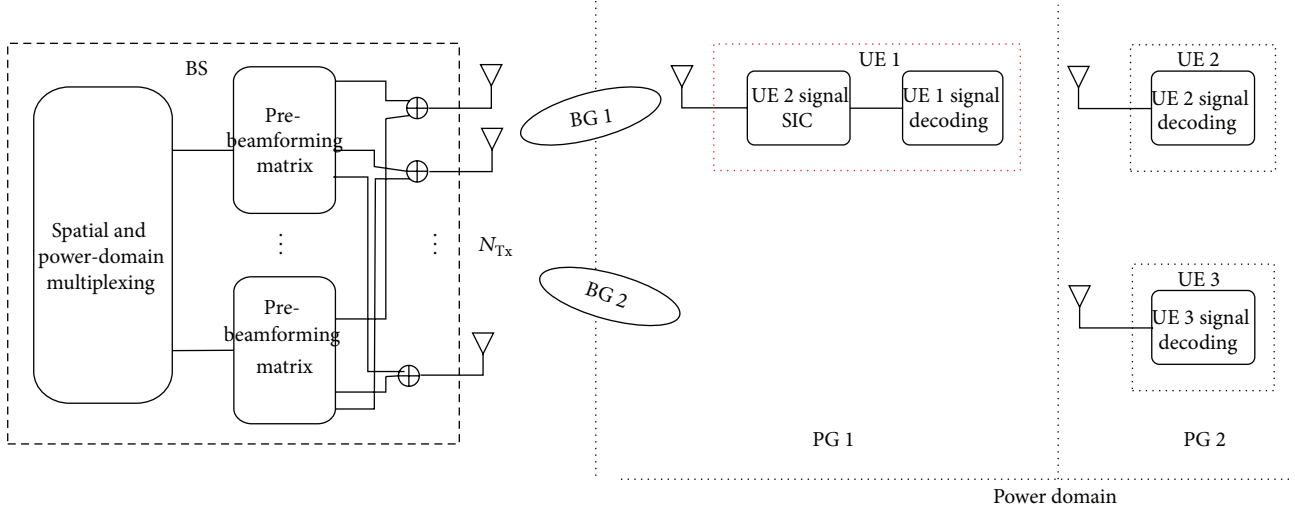


FIGURE 2: Power-domain multiplexing BS-UE transceiver diagram.

TABLE 1: Computational complexity comparison.

Numbers of complex number addition and multiplication	JSDM	JSPM with fix power user paring algorithm	JSPM with power domain greedy algorithm
Prebeamforming		$G \times O(N_t^3) + G \times U^g \times M_B^g \times N_t$	
Multuser precoding		$G \times O((U^g)^3) + G \times U^g \times r^g \times M_B^g$	
Power domain user paring		$U_{m,d}^g \times U_{m,d'}^g \times G \times O((r^g)^2)$	$C_{(U_{m,d}^g + U_{m,d'}^g)}^2 \times G \times O((r^g)^2)$
Power domain multiplexing		$U^g \times r^g \times G$	$U^g \times r^g \times G$

center user group and cell edge user group; numbers of the two groups of UE are noted as  $U_{m,d}^g$  and  $U_{m,d'}^g$  respectively. The computational complexity of JSPM and JSDM in BS side is presented in Table 1.

From Table 1, we can see that although the power-domain multiplexing transmission of JSPM leads to computational complexity increase, the added complexity accounts for a small part of the overall JSPM complexity. The main computational complexity comes from the singular value decomposition (SVD) processing of channel matrix  $\mathbf{H} = [\mathbf{H}^1 \dots \mathbf{H}^G]$  with  $O(N_t^3)$  computational complexity in multuser beamforming procedure. Therefore the extra complexity introduced by adopting JSPM has very limited impact on the overall system implementation.

From computational complexity listed in Table 1, we can see that the approach of predefined user grouping and per-group fixed power allocation has more less computational complexity, compared with greedy algorithm, with the cost of little performance degradation which we will discuss in Section 4.

For UE side, the detection complexity of cell center UE will not change, the detection complexity of cell edge UE will be double because for cell edge UE; they will firstly detect the information of cell center pairing UE and subtract it from receiving signals and then detect its own information. However, 3GPP RAN4 has finished SIC performance requirement in 3GPP TS36.101 [19], which means that Rel.12 UE

has enough capability to fulfill the detection performance requirement of JSPM.

## 4. Performance Evaluation and Analysis

**4.1. Validation of the Asymptotic Analysis.** In this section, we compare the results obtained via the method of deterministic equivalents with Monte Carlo simulations in order to validate the asymptotic analysis in Section 2.

In our discussion, BS is equipped with a uniform circular array with 100 isotropic antenna elements; the distance between antenna elements equals  $\lambda/2$ , where  $\lambda$  is the carrier wavelength. As the user mutual statistical independent channel is important for analytical results, the one-ring channel model [11] is adopted. Users form  $G = 6$  symmetric spatial groups with the angular spread (AS)  $\Delta = 15^\circ$  and azimuth  $\text{AOA}\theta_g = -\pi + \Delta + (g-1)(2\pi/G)$ ,  $g = 1, \dots, G$ .

We fixed to serve  $r^g = 5$  data streams per spatial group, so that the total number of active users is 30.  $I_m^g$  is fixed to equal 2. SNR = P with the noise unit variance normalization.

The comparison of sum spectrum efficiencies of JSPM obtained by using deterministic equivalent approximation and simulations is illustrated in Figure 3. The green solid line with "squares" is obtained using the JSPM corresponding deterministic equivalent approximation, the red solid line with "x" is obtained through JSPM simulation, and the blue solid line with "o" is obtained through JSDM simulation.

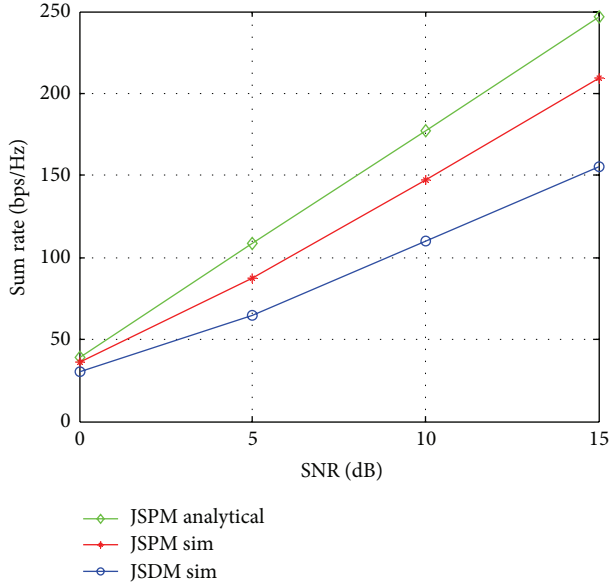


FIGURE 3: Comparison of sum spectrum efficiencies.

For multiuser spatial transmission simulation, the approach of ZF beam-forming (ZFBF) and joint group processing (JGP) is used. For multiuser transmission of power-domain simulation, the predefined user grouping and per-group fixed power allocation scheme in power-domain is applied.

As shown in Figure 3, the trend of JSPM simulation result is coincided with that of JSPM deterministic equivalent approximation. Furthermore simulation results show that the performance of JSPM outperforms JSDM.

**4.2. JSPM Performance Gain.** In this section, we present system-level simulation results of the investigation on the performance gains of JSPM in LTE system. In our simulation, a multicell system-level simulation is conducted and a 19-hexagonal macro cell model with 3 cells per cell site is employed. The details of the simulation assumptions are listed in Table 2.

BS is equipped with antenna array of  $8 \times 8$  X-pol elements, as shown in Figure 4. For the simulation, there are 2 vertical prebeamforming groups by using prebeamforming matrix  $\mathbf{B}$ , columns of which can be 4-element DFT weight; the high beam group is tilted to 80 degrees, and the low beam group is tilted to 100 degrees. Therefore UE in serving cell can be partitioned into two vertical spatial groups by BS based on UE RSRP measurement and feedback responding to two vertical antenna ports; each vertical antenna port is mapped to four vertical rows of antenna elements with one polar direction, such as  $+45^\circ$  polar, as shown in Figure 4. Then BS can apply MU-MIMO transmission for UE in each vertical group by using matrix  $\mathbf{V}$ . Matrix  $\mathbf{V}$  can be composed with UE feedback precoding matrix index for eight horizontal antenna ports. UE gets the horizontal channel spatial information by measuring the horizontal CSI-RS ports. In the simulation, the one horizontal antenna port is mapped to two columns of antenna elements of one polar direction; for example, port 0

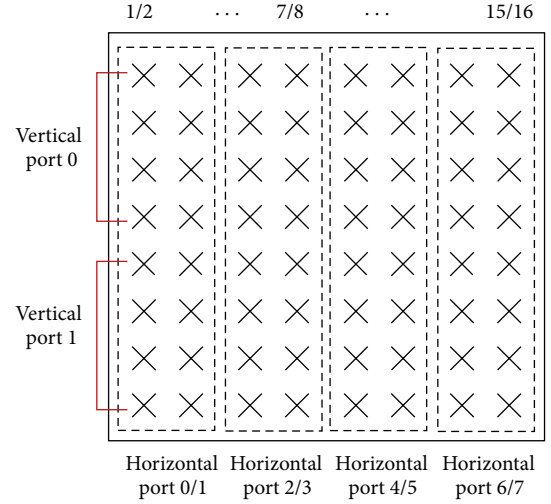
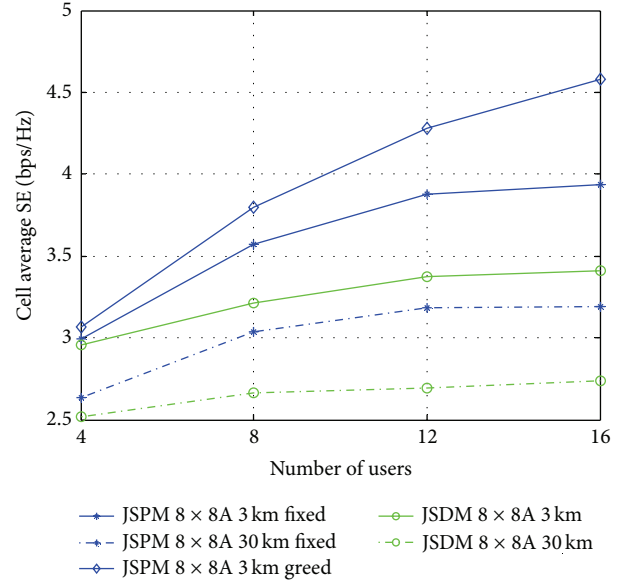
FIGURE 4: Antenna array with  $8 \times 8$  X-pol elements.

FIGURE 5: Cell average spectrum efficiency (SE) comparison with different user numbers per cell.

is mapped to column 1 and 3 of  $+45^\circ$  polar antenna elements, as shown in Figure 4. In simulation, the fix power-domain grouping scheme is adopted, the threshold for predefined user grouping is 8 dB, and the power ratio is (0.3P, 0.7P).

Figure 5 shows the cell average spectrum efficiency (in bits/sec/Hz) of JSDM and JSPM versus the number of users in the system. The results show that JSPM can achieve higher cell average spectrum efficiency (more than 15% gain with 16 users per cell and 3 km/h velocity condition) than JSDM as JSPM can achieve additional power-domain multiplexing gain. The ratio of UE multiplexing in spatial and power domain for different amounts of UE per cell are summarized in Table 3. From Table 3, it can be seen that as the amount of UE per cell is increased, the ratio of UE multiplexing in spatial and power domain is increased and the ratio of

TABLE 2: Major simulation parameters.

Parameters	Values
Tx power	46 dBm for 3D-UMa 500 m
Duplex	FDD
BS antenna configurations	Antenna elements config: $8 \times 8 \times 2 (\pm 45)$ , $0.5\lambda H/0.8\lambda V$
Traffic model	Full buffer model
Wrapping method	Geographical distance based
Metrics	5%, 50% UPT
System bandwidth	10 MHz (50 PRBs)
UE attachment	Based on RSRP
Number of UEs per cell	4/8/12/16
Network synchronization	Synchronized
UE speed	3 km/h
UE distribution	According to 36.873 [20]
Receiver	Nonideal channel estimation and interference modeling, detailed guidelines according to Rel-12 assumptions MMSE-IRC and IC receiver, and detailed guidelines according to Rel-12 assumptions [21]
UE Rx antenna configuration	1 Rx
Feedback	PUSCH 3-2 CQI, PMI, and RI reporting triggered per 5 ms Feedback delay is 5 ms Rel-10 8 Tx codebook
Transmission scheme	Dynamic SU/MU-MIMO with rank adaptation
Overhead	3 symbols for DL CCHs, 2 CRS ports, and DM-RS with 12 REs per PRB
CSI-RS	5 msec
SRS	1 Tx, 5 ms periodicity, wideband

TABLE 3: Ratio of UE multiplexing comparison for different UE numbers per cell.

Number of UEs per cell	Ratio of UE multiplexing of JSPM [%]	Ratio of UE multiplexing of JSMD [%]
4	30.2%	28.4%
8	43.9%	37.2%
12	49.6%	41.4%
16	50.7%	43.7%

UE multiplexing is about 30% when the number of UEs per cell is 4, while the ratio of UE multiplexing increases to approximately 50% when the amount of UE is 16. Therefore the gain of JSPM is also increased as shown in Figure 5.

The performances of JSPM and JSMD with UE speed 30 km/h are also provided in Figure 5. These results indicate that the performances of JSPM and JSMD both decrease with UE speed increasing. For JSPM, the performance loss is about 19% when UE speed increases from 3 km/h to 30 km/h with 16 users per cell since UE mobility causes the rapid channel change and reduces the BS channel estimation accuracy. Therefore JSPM scheme is more suitable for a stationary or

semistationary scenario, such as to provide coverage and high data rate for users in office rooms or tall buildings.

For the sake of performance comparison of different power-domain user pairing strategies, we also provide the performance of JSPM with fixed power user pairing selection (denoted as blue solid line with “\*”) and greedy user pairing selection (denoted as blue solid line with square) in Figure 5. Although the performance loss of fixed power user pairing compared with greedy user pairing is about 15% with 16 users per cell and 3 km/h velocity condition, the fixed power user pairing algorithm can provide less computational complexity and easier system implementation than greedy algorithm, as discussed in Section 3.3; hence it will be the preferred method for practical user pairing in BS side.

**4.3. Different Antenna Type Performances.** In this subsection, we perform JSPM performance evaluation for two antenna types with  $8 \times 8$  and  $4 \times 16$  X-polar antenna elements, respectively. As the typical application scenario of massive MIMO is providing high-speed data service for users in tall buildings, the vertical grouping scheme, which has been discussed in the above section, is adopted for both  $8 \times 8$  X-polar and  $4 \times 16$  X-polar antenna types in the simulation. For the antenna array with  $4 \times 16$  X-polar antenna elements, there are 2 vertical prebeamforming groups by using



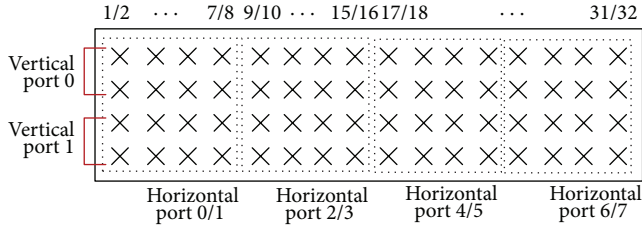
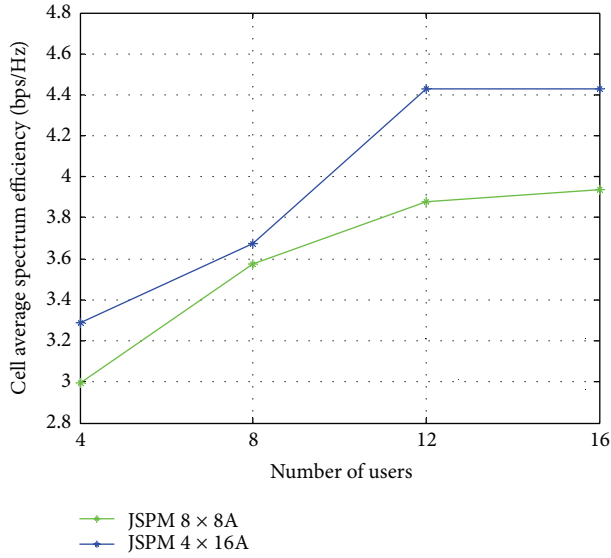
FIGURE 6: Antenna array with  $4 \times 16$  X-pol elements.

FIGURE 7: Cell average spectrum efficiency (SE) comparison with different user numbers per cell.

prebeamforming matrix  $\mathbf{B}$ , columns of which can be 2-element DFT weight; two beam groups are tilted to 80 and 100 degrees, respectively. Two vertical antenna ports are mapped to four vertical rows of antenna elements with one polar direction; each one is corresponding to two rows. For eight horizontal antenna ports, each horizontal antenna port is mapped to four columns of antenna elements of one polar direction, for example, port 0 is mapped to column 1/3/5/6 of  $+45^\circ$  polar antenna elements as shown in Figure 6.

In the simulation, the other schemes, such as user spatial grouping scheme, MU-MIMO scheme, and multiuser power-domain transmission scheme, are the same as that mentioned in previous section.

Figure 7 shows the cell average spectrum efficiency comparison between two types of antenna array. Figure 8 gives the CDF comparison of UE spectrum efficiency between two types of antenna array with 4/8/12/16 UEs per cell. Based on these results, it can be seen that the  $4 \times 16$  antenna array has better performance than the  $8 \times 8$  antenna array both in cell average spectrum efficiency and in 50% CDF of UE spectrum efficiency. This is because that BS with  $4 \times 16$  antenna array, which has more horizontal column antennas, can form narrower beams and separates the spatial channel into more subpace; therefore it can achieve more spatial multiplexing gain.

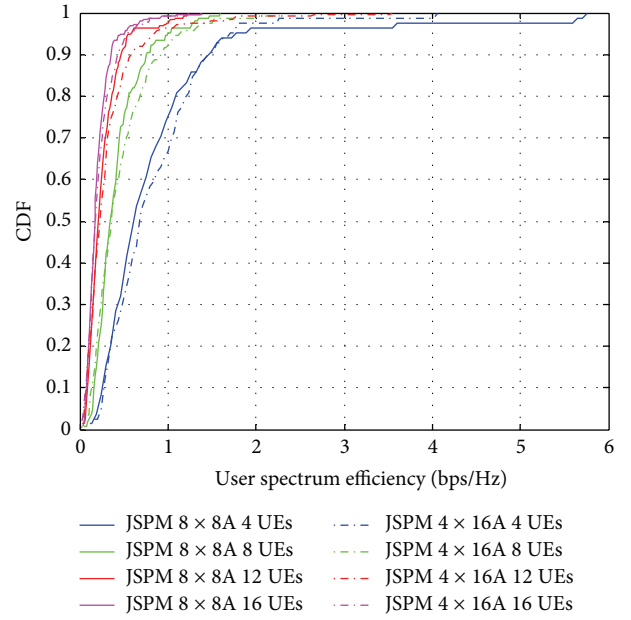


FIGURE 8: CDF of UE spectrum efficiency.

It can be also seen that the antenna array with more column antennas can achieve higher multiplexing gain for JSPM scheme with number limitation of antenna elements in the practical network.

## 5. Conclusion

In this paper, a joint spatial and power-domain multiuser transmission scheme, called JSPM, is proposed for FDD massive MIMO systems. In this scheme, BS divides the UE into different groups in spatial and power domains, and each type of UE is identified with a set of indices including spatial domain index, beam index, and power-domain index. Based on these UE indices, BS can perform multiuser pairing and scheduling in both spatial and power domain. Compared with the traditional spatial multiplexing schemes, the proposed JSPM scheme can achieve additional power-domain multiplexing gain. The system-level simulation results validate that, with 16 users per cell, JSPM can achieve more than 15% spectrum efficiency gain compared with JSDM, and the JSPM gain increases with the number of active users per cell. The simulation results also show that the antenna array with larger number of horizontal column antennas has the better performance, since user distribution in the horizontal plane is more intensive than that in the vertical plane in practical networks.

## Conflict of Interests

The authors declare that there is no conflict of interests regarding the publication of this article.

## References

- [1] E. G. Larsson, O. Edfors, F. Tufvesson, and T. L. Marzetta, "Massive MIMO for next generation wireless systems," *IEEE Communications Magazine*, vol. 52, no. 2, pp. 186–195, 2014.
- [2] T. L. Marzetta, "Noncooperative cellular wireless with unlimited numbers of base station antennas," *IEEE Transactions on Wireless Communications*, vol. 9, no. 11, pp. 3590–3600, 2010.
- [3] K. Zheng, L. Zhao, J. Mei, B. Shao, W. Xiang, and L. Hanzo, "Survey of large-scale MIMO systems," *IEEE Communications Surveys & Tutorials*, vol. 17, no. 3, pp. 1738–1760, 2015.
- [4] K. Zheng, Y. Wang, W. Wang, M. Dohler, and J. Wang, "Energy-efficient wireless in-home: the need for interference-controlled femtocells," *IEEE Wireless Communications*, vol. 18, no. 6, pp. 36–44, 2011.
- [5] J. Jose, A. Ashikhmin, T. L. Marzetta, and S. Vishwanath, "Pilot contamination and precoding in multi-cell TDD systems," *IEEE Transactions on Wireless Communications*, vol. 10, no. 8, pp. 2640–2651, 2011.
- [6] H. Huh, A. M. Tulino, and G. Caire, "Network MIMO with linear zero-forcing beamforming: large system analysis, impact of channel estimation, and reduced-complexity scheduling," *IEEE Transactions on Information Theory*, vol. 58, no. 5, pp. 2911–2934, 2012.
- [7] G. Caire, N. Jindal, M. Kobayashi, and N. Ravindran, "Multiuser MIMO achievable rates with downlink training and channel state feedback," *IEEE Transactions on Information Theory*, vol. 56, no. 6, pp. 2845–2866, 2010.
- [8] M. Kobayashi, N. Jindal, and G. Caire, "Training and feedback optimization for multiuser MIMO downlink," *IEEE Transactions on Communications*, vol. 59, no. 8, pp. 2228–2240, 2011.
- [9] A. Adhikary, J. Nam, J.-Y. Ahn, and G. Caire, "Joint spatial division and multiplexing: the large-scale array regime," *IEEE Transactions on Information Theory*, vol. 59, no. 10, pp. 6441–6463, 2013.
- [10] J. Nam, J.-Y. Ahn, A. Adhikary, and G. Caire, "Joint spatial division and multiplexing: realizing massive MIMO gains with limited channel state information," in *Proceedings of the 46th Annual Conference on Information Sciences and Systems (CISS '12)*, Princeton, NJ, USA, March 2012.
- [11] J. Nam, A. Adhikary, J.-Y. Ahn, and G. Caire, "Joint spatial division and multiplexing: opportunistic beamforming, user grouping and simplified downlink scheduling," *IEEE Journal on Selected Topics in Signal Processing*, vol. 8, no. 5, pp. 876–890, 2014.
- [12] V. Venkateswaran and A.-J. van der Veen, "Analog beamforming in MIMO communications with phase shift networks and online channel estimation," *IEEE Transactions on Signal Processing*, vol. 58, no. 8, pp. 4131–4143, 2010.
- [13] K. Zheng, L. Zhao, J. Mei, M. Dohler, W. Xiang, and Y. Peng, "10 Gb/s hetsnets with millimeter-wave communications: access and networking-challenges and protocols," *IEEE Communications Magazine*, vol. 53, no. 1, pp. 222–231, 2015.
- [14] O. E. Ayach, R. W. Heath Jr., S. Abu-Surra, S. Rajagopal, and Z. Pi, "Low complexity precoding for large millimeter wave MIMO systems," in *Proceedings of the IEEE International Conference on Communications (ICC '12)*, pp. 3724–3729, Ottawa, Canada, June 2012.
- [15] A. Alkhateeb, O. El Ayach, G. Leus, and R. W. Heath, "Hybrid precoding for millimeter wave cellular systems with partial channel knowledge," in *Proceedings of the Information Theory and Applications Workshop (ITA '13)*, pp. 1–5, IEEE, San Diego, Calif, USA, February 2013.
- [16] D. Tse and P. Viswanath, *Fundamentals of Wireless Communication*, Cambridge University Press, Cambridge, UK, July 2005.
- [17] M. Sharif and B. Hassibi, "On the capacity of MIMO broadcast channels with partial side information," *IEEE Transactions on Information Theory*, vol. 51, no. 2, pp. 506–522, 2005.
- [18] A. Benjebbovu, A. Li, Y. Saito, Y. Kishiyama, A. Harada, and T. Nakamura, "System-level performance of downlink NOMA for future LTE enhancements," in *Proceedings of the IEEE Globecom Workshops (GC '13)*, pp. 66–70, IEEE, Atlanta, Ga, USA, December 2013.
- [19] 3GPP TS36.101 (V13.1.0), "Evolved Universal Terrestrial Radio Access (E-UTRA); User Equipment (UE) radio transmission and reception," October 2015.
- [20] 3GPP TR36.873 (V12.2.0), "Study on 3D channel model for LTE," July 2015.
- [21] 3GPP, "Study on network-assisted interference cancellation and suppression (NAIC) for LTE," 3GPP TR36.866 (V12.0.1), 2014.

